Thermodynamics and Kinetics of Coal Gasification in a Liquid Iron Bath

I. BARIN, M. MODIGELL, and F. SAUERT

The thermodynamics and kinetics of the Molten-Iron–Pure-Gas (MIP) process used for coal gasification have been analyzed. In the MIP process, oxygen, fine-grained coal, and fluxes are injected into a liquid iron bath to produce a high temperature gas consisting of CO and H_2 plus a liquid basic slag. The sulfur is transferred from the coal to this slag. Computer calculations bearing in mind test conditions were used to determine equilibrium conditions as well as mass and energy balances; these indicated that the MIP process is technically feasible. The kinetics of the gasification process have been investigated by analyzing and assessing the basic reactions for a bottom-blowing MIP reactor. A comparison of all relevant reactions reveals that the dissolution of carbon in iron is the rate-determining step of the process. The bath turbulence induced by the injected gas and by the product gas results in intense mixing and dispersion of the reactants and their intermediate products. These phenomena create extremely large mass-transfer surfaces and extend the retention time of the reactants in the liquid iron bath. This results in high conversion rates relative to the volume of the MIP reactor.

I. INTRODUCTION

THE gasification of coal for generating a gas consisting predominantly of CO and H_2 has been practiced for a long time. For decades, efforts have been made to improve existing gasification processes and to develop new ones. A more recent method for gasifying coal is the "MIP" (Molten-Iron–Pure-Gas) process, in which oxygen gas, fine-grained coal and fluxes are either injected into a liquid iron bath[1,2,3] or blown perpendicularly onto the bath surface.[4,5] The process produces a low-sulfur gas consisting primarily of CO and H_2 at temperatures of 1650 to 1800 K. The sulfur present in the coal is transferred together with the ash-forming constituents to a liquid slag. Coal gasification in liquid iron combined with iron- and steelmaking is another line of development tested by other investigators.[6–9]

The important factors governing the MIP process have been studied during preliminary investigations.[2,5] Development work is continuing with systematic tests now being carried out in a recently installed pilot-plant reactor at Luleå, Sweden. The cylindrical reactor (3 m diameter × 6 m long) lies horizontally and input materials (oxygen, coal, and limestone) can be injected by either bottom- or top-blowing techniques with operating pressures of up to 3×10^5 Pa.

Basic research on coal gasification in a liquid iron bath has not yet been carried out. However, certain aspects of the physical chemistry of steelmaking can be applied to liquid iron bath gasification. From this standpoint, the present paper describes calculations of the thermodynamics and kinetics of the MIP process for the bottom-blowing reactor, including some comparison with preliminary results.

II. THERMODYNAMICS

A. *Basis of Calculations*

For thermodynamic calculations, coal gasification in a liquid iron bath is considered as a steady-state flow process in an isothermal-isobaric reactor. As shown schematically in Figure 1, coal, oxygen, and other feed materials are considered as reacting with each other in the reactor until equilibrium or a defined approach to equilibrium has been reached. The product gas containing dust is assumed to leave the reactor continuously, with the liquid slag being withdrawn either continuously or batchwise.

The equilibrium phases and main components contained in the reactor may be represented by:

liquid iron bath: Fe, C, S, Si;
slag : CaO, CaS, SiO_2, Al_2O_3, K_2O, MgO;
gas phase : CO, H_2, CO_2, H_2S, CH_4.

In this paper the liquid iron bath has, for reasons of simplicity, been assumed to be an Fe-C-S alloy. Slag constituents have been considered to be simple compounds instead of ions. The gas phase has been assumed to be ideal.

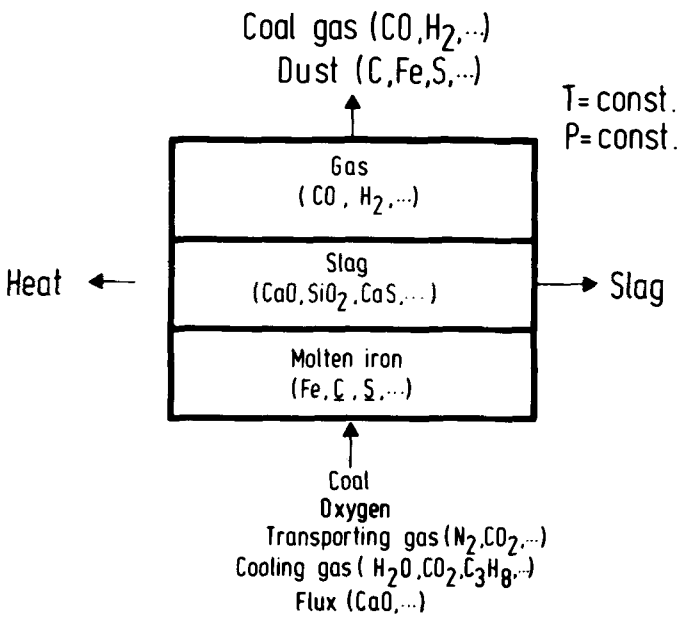

Fig. 1 — Schematic representation of coal gasification in the liquid iron bath as a stationary flow process.

I. BARIN, Head, and M. MODIGELL and F. SAUERT, Senior Project Managers, are with Basic Research and Development, KHD Humboldt Wedag AG, 5000 Cologne 90, West Germany.

Manuscript submitted June 9, 1986.

Apart from the three equilibrium phases mentioned, mass and energy balances must account for the dust entrained in the product gas. The composition and quantity of the dust have been based on test results. Similar considerations apply to the dissolution of the reactor brick lining during gasification. The overall process is autothermal. The heat transfer from the reactor to its environment is balanced by the net reaction enthalpy so that a constant temperature profile is assumed.

Thermodynamic calculations were performed with the aid of computer programs and data base including Eriksson's SOLGASMIX program.[11] Quantities and ratios of feed materials necessary for the desired product compositions were ascertained by iterative variations.

B. *Thermochemical Data*

The thermochemical data for pure substances were acquired from data compilations.[12,13] The activity coefficients of the components of the Fe-C-S system have been calculated using equations from the quadratic formalism introduced by Darken.[14,15a] The activity a_i of the component i is defined as,

$$a_i = X_i \gamma_i \qquad [1]$$

where X_i denotes the atom (mole) fraction and γ_i the activity coefficient. From equations and parameters given in Reference 14 the following relations have been derived for the concentration range:

$$0.05 < X_C < 0.2 \quad \text{and} \quad X_S < 0.001 \text{ at } T = 1773 \text{ K}:$$

$$\log \gamma_{Fe} = -2.51X_C^2 - 3.66X_C X_S \qquad [2]$$

$$\log \gamma_C = -2.51[(1 - X_C)^2 - (1 - X_C^{sat})^2] - \log X_C^{sat} \qquad [3]$$

$$\log \gamma_S = -2.51X_C^2 + 3.66X_C - 1.67X_S \qquad [4]$$

The standard states are pure liquid iron for Fe, graphite for C, and infinite dilute solution for S. γ_S stands for the ratio of the activity coefficient γ_S' of S in the Fe-C-S system and the Henrian coefficient γ_S° in the Fe-S system, *i.e.*, $\gamma_S = \gamma_S'$ (Fe-C-S)/γ_S°(Fe-S). The numerical coefficients in Eqs. [2], [3], and [4] have been calculated by temperature shift of values specified in Reference 14 with the assumption that the coefficients were inversely proportional to T.[16] X_C^{sat} in Eq. [3] denotes the mole fraction of C at graphite saturation of liquid Fe and is represented by the following relation:[17]

$$\log X_C^{sat} = -560/T - 0.375 \qquad [5]$$

Equations [2] and [3] apply for a relatively wide concentration range leading to activity values which are in satisfactory accord with experimental data.[18,19] Sulfur activities calculated using Eq. [4] in combination with solution data from the binary Fe-S system[20,21] are in agreement with the experimental data from the ternary Fe-C-S system.[22]

Accurate data for the activity coefficients of the slag components are not available. To determine the equilibrium concentration of S in the liquid slag, the following relations were used:

$$O^{2-}(\text{slag}) + \frac{1}{2}S_2(\text{gas}) = S^{2-}(\text{slag}) + \frac{1}{2}O_2(\text{gas}), \qquad [6a]$$

$$C_S = (\text{wt pct S})_{\text{slag}} (P_{O_2}/P_{S_2})^{1/2} \qquad [6b]$$

In Eq. [6b] C_S is the sulfur capacity for which the following relation was derived from the data reported by Venkatradi and Bell[23] at $T = 1773$ K:

$$\log C_S = 1.38 \frac{X_{CaO} + X_{MgO}/2}{X_{SiO_2} + X_{Al_2O_3}/3} - 5.59 \qquad [7]$$

After calculation of gas-iron bath equilibrium, X_{CaO} was determined *via* the amount of CaO (lime input) by iterative variations using Eqs. [6] and [7] until sulfur equilibrium was reached, with allowance being made for the mass balance.

C. *Calculation Parameters and Results*

The following conditions were assumed for the calculations: $T = 1773$ K, $P = 10^5$ Pa, wt pct C (dissolved in Fe) = 3.5, total S content of product gas = 100 vol ppm. Further data, such as the composition of coal and other feed materials, the quantity and composition of the entrained dust, and the reactor heat losses, were taken from preliminary tests with a converter containing 3000 kg Fe.[2] The specific reactor throughput was assumed to be 500 kg coal per hour and 1000 kg liquid iron bath.

Table I presents the overall mass and enthalpy balance related to a throughput of 1000 kg of coal. For the case under discussion, the net enthalpy for the reactions was calculated to be −0.160 GJ corresponding to the heat losses of the reactor to the environment. For a given product quality, the energy balance is strongly influenced by the composition of the feed materials, in particular by the composition of the coal. In special cases, depending on the calorific value of the feed coal, preheated air or preheated oxygen-air mixtures instead of pure oxygen may be used as gasification agent.

The compositions of the feed coal and entrained dust are given in Table IIa. Table IIb shows the compositions of the produced slag and gas phase for the equilibrium state at 10^5 Pa and 1773 K. The gas phase consists mainly of CO

Table I. Mass- and Enthalpy Balance Based on a Coal Throughput of 0.278 kg s^{-1} (= 1 Metric Ton Per Hour) (Gas Volume at Standard State)

Material		Enthalpy H (GJ)
Input (298 K)		
Coal	1000.0 kg	−1.214
Lime	85.8 kg	−0.982
Oxygen	742.9 m^3	0.
Transport gas (N_2)	100.0 m^3	0.
Cooling gas (C_3H_8)	74.3 m^3	−0.344
Steam (H_2O, 673 K)	179.0 m^3	−1.826
Iron (1773 K)	23.1 kg	0.029
Bricklining (1773 K)	0.5 kg	−0.005
		−4.342
Output (1773 K)		
Product gas	2606.5 m^3	−3.002
Slag	158.9 kg	−1.568
Dust	65.9 kg	0.068
		−4.502
Reaction enthalpy:		
H (output) − H (input)		−0.160

Table IIa. Composition of Feed Coal and Entrained Dust

Feed Coal		Dust	
	Wt Pct		Wt Pct
C	84.0	C	55.4
H	2.6	Al_2O_3	0.26
N	1.0	CaO	0.03
O	3.1	Fe	13.3
S	0.8	Fe_2C	12.2
Al_2O_3	2.51	FeS	4.9
CaO	0.12	Fe_2O_3	12.5
Fe_2O_3	0.44	K_2O	0.5
K_2O	0.34	MgO	0.05
MgO	0.11	Na_2O	0.32
Na_2O	0.17	SiO_2	0.64
P_2O_5	0.05		
SiO_2	3.66		
SO_3	0.1		

Table IIb. Equilibrium Composition of Produced Slag and Gas Phase at $P = 10^5$ Pa and $T = 1773$ K

Slag		Product Gas		
	Wt Pct			
C	0.01	CO	66	vol pct
Al_2O_3	16.1	H_2	29.8	vol pct
Cao	43.5	N_2	4.1	vol pct
CaS	9.9	H_2O	154	vol ppm
FeO	1.9*	CO_2	90	vol ppm
K_2O	2.0	H_2S	53	vol ppm
MgO	1.3	CS	42	vol ppm
MnO	0.05	CH_4	29	vol ppm
Na_2O	1.0	COS	5	vol ppm
P_2O_5	0.3	rest	627	vol ppm
SiO_2	24.0			
		Partial Pressures		
*Nonequilibrium value		O_2: 4.7×10^{-11} Pa		
		S_2: 2.3×10^{-3} Pa		

and H_2 besides 4.1 vol pct N_2. Corresponding to the gas composition with $P_{O_2} = 4.7 \times 10^{-11}$ Pa the C content in the iron bath is 3.5 wt pct. Under these conditions, the slag will also contain carbon;[24] however, data for C solubility in slags of desired composition are not available. For the mass balance calculations the total C content of the slag has been assumed to be 0.01 wt pct. The FeO activity of the slag was calculated as 4.5×10^{-4}. The corresponding FeO content may be estimated as 0.05 wt pct assuming $a_{FeO} \approx X_{FeO}$[23] and inserting $X_{FeO} = 0.009 \times$ wt pct FeO. However, for the mass and enthalpy balance, the FeO content of the slag was assumed to be 1.9 wt pct, because during gasification a certain proportion of the initially formed FeO is mechanically transferred to the slag.

The effects of temperature, pressure, and C content of the liquid iron bath on the composition of the product gas are shown in Figures 2(a), 2(b), and 2(c) with reference to the gas composition prevailing at 10^5 Pa, 1773 K, and 3.5 wt pct C.

For the equilibrium state with 100 vol ppm S in the gas phase, the S content in the slag and in liquid iron was calculated to be 4.4 wt pct and 0.03 wt pct, respectively. The corresponding S distribution between slag and iron bath, wt pct S (slag)/wt pct S (iron) = 147, is nearly the same as the equilibrium distribution of S between graphite-

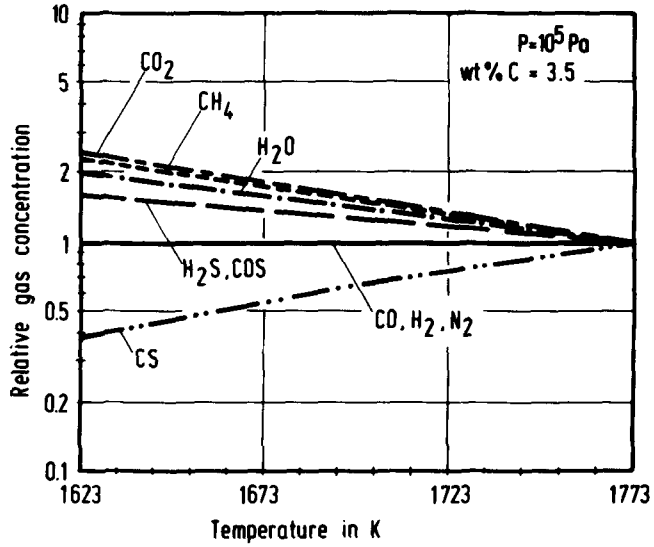

(*a*)

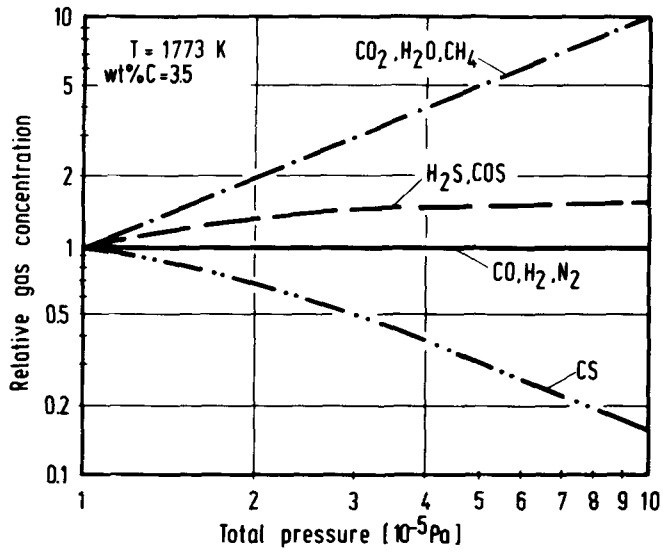

(*b*)

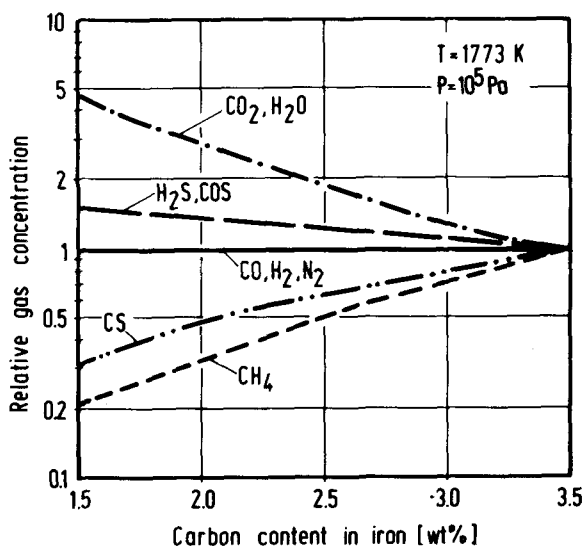

(*c*)

Fig. 2 — Change of equilibrium composition of the product gas as a function of temperature (*a*), pressure (*b*), and carbon content of the liquid iron bath (*c*) relative to the gas composition at 1773 K, 10^5 Pa, and 3.5 wt pct C.

saturated liquid iron and blast-furnace-type slags containing 10 to 20 wt pct Al_2O_3.[26b,27] Here, data given in Reference 26b were extrapolated for comparison. Figure 3 shows the S distribution between the liquid iron bath and the gas phase without consideration of the slag. Figure 4 depicts the change of the S content in the gas phase with the slag basicity defined by B = wt pct CaO/wt pct SiO_2. From this figure it follows that for the process requirements chosen, B is found to be 1.81. As can be seen from Figure 5 derived from experimental data,[25,26a] a liquid slag is formed.

On cooling the product gas for dust removal and further treatment, the gas composition will change with decreasing temperature. One of the reactions occurring is the carbon deposition *via* CO decomposition which has not been observed during recent tests. This is probably the result of quick cooling. Depending on particular conditions in the heat recovery system, the sulfur content of the gas phase decreases as a result of reactions of S-containing gas components with iron dust forming FeS.[8] This effect explains the low S content of 20 vol ppm found in the product gas during the tests.[2,10]

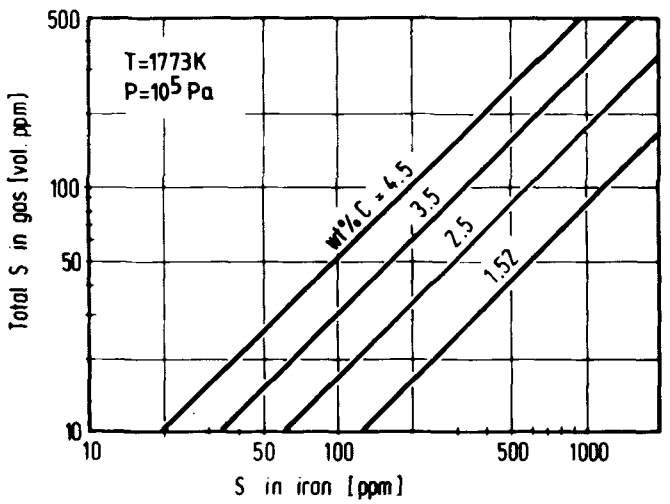

Fig. 3 — Total calculated sulfur content of gas phase as a function of sulfur content in liquid iron for different carbon concentrations in equilibrium state at 1773 K and 10^5 Pa.

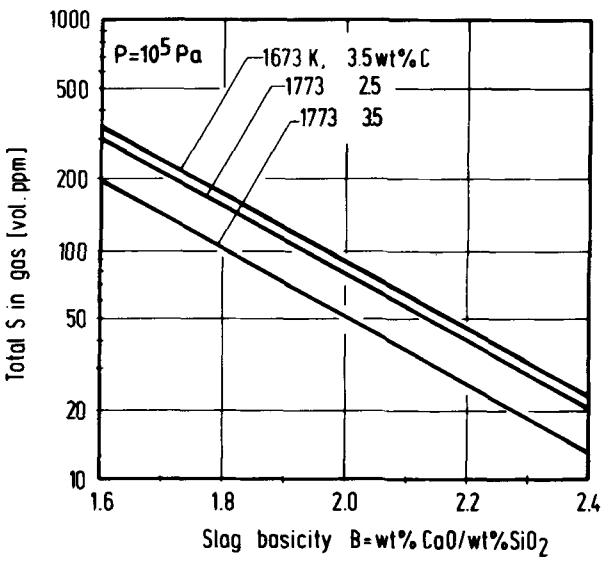

Fig. 4 — Total calculated sulfur content of gas phase as a function of slag basicity for different carbon concentrations in liquid iron in equilibrium state at 10^5 Pa.

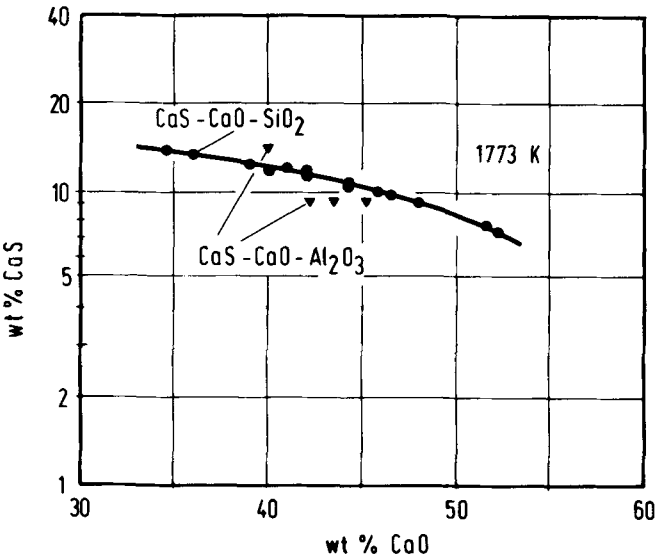

Fig. 5 — Solubility of CaS in calcium silicate and calcium aluminate melts at 1773 K.[25,26a]

For the example considered here, the following mass ratio resulted for the sulfur distribution:

$$\text{slag/dust/liquid iron/gas} = 1/0.17/0.09/0.05.$$

Thermodynamic calculations have revealed that minority gas components, such as HCN, alkali metals, and halogens are either decomposed as a result of reactions at lower temperatures, or are converted to condensed phases. The latter would also apply to metals such as Zn, Cd, and Pb if they are contained in the input materials. Such metals will leave the reactor as metallic fumes and can be separated as chalcogenides at lower temperatures.

The equilibrium calculations are essentially confirmed during the tests.[2,10] The thermodynamic calculation presented here will serve primarily for defining possibilities and limitations associated with the MIP process.

III. KINETICS OF THE REACTIONS OF COAL AND OXYGEN

A number of interconnected reactions take place in the liquid iron bath reactor. The discussion here will deal only with the kinetics of essential reactions under simplified conditions and will assess their effect on the overall process. The hydrodynamic phenomena in the liquid iron bath will be discussed separately later.

In the bottom-blowing reactor, feed materials are injected into the liquid iron bath through bottom tuyeres. The blowing parameters are adjusted so that a liquid-free gas space is formed above the tuyeres; consequently the injection nozzles operate in the "jet flow regime". At the interface of this space, which is continuously changing in shape and size, high temperatures result from the initial oxidation of the liquid iron. The pyrolysis of coal and other oxidation reactions also commence within this injection zone.

The injecting gas also generates gas bubbles of varying dimension, which undergo further reactions, again associ-

ated with the generation of new gas bubbles, and which finally leave the liquid iron bath as a product gas. The movement of the gas bubbles induces intense turbulence in the liquid iron bath, thereby widely dispersing the reactants. The turbulence enlarges the mass transfer region and extends the retention time of the reactants, thus explaining the high specific conversion rates attained in liquid iron bath reactors.

A. *Heating-Up and Dissolution of Coal Particles*

The reactions will be discussed in the following as isolated phenomena, applicable in case of spherical coal particles of 1 mm diameter and a carbon content of 84 wt pct (Table IIa) which enter the reactor with a velocity of 100 m/s.

Coal particles introduced into the iron bath reactor first pass through the gas space over the bottom-tuyeres and then impinge on the iron melt. Water-model tests estimate that the average height of the gas space above the tuyere is approximately 10 cm. Consequently, the retention time of the particles within that gas space is about 10^{-3} second. The oxygen-coal reactions will thus be very limited and carbon conversion will occur primarily within the liquid iron.

The terminal velocity of coal particles in the liquid iron bath may be estimated using the equation of motion in combination with the following relation for the drag coefficient C_d for rigid spheres:[28]

$$C_d = \frac{24}{\mathrm{Re}} + \frac{3.73}{\mathrm{Re}^{1/2}} - \frac{0.0048\ \mathrm{Re}^{1/2}}{1 + 3 \times 10^{-6}\ \mathrm{Re}^{3/2}} + 0.49 \qquad [8]$$

where Re denotes the Reynolds number. Thus a coal particle of 1 mm diameter with a density of 1.3 g/cm^3, entering the liquid iron with an initial velocity of 100 m/s, will achieve a terminal velocity of 11 cm/s within 6×10^{-3} s.

The liquid iron bath heats the coal particles rapidly as determined from simplified heat transfer calculations using nomograms for temperature change in inert spheres surrounded by fluids of constant temperature.[29] The course of temperature in the center of a coal particle of 1 mm diameter is shown in Figure 6. For the calculation of the heating curve the following assumptions were made: temperature of liquid iron = 1773 K, initial temperature of coal = 298 K, thermal conductivity of coal = 1.6×10^{-2} cm^2/s, and Nusselt number (Nu) = 2. As shown in Figure 6, the center of the coal particle reaches 90 pct of the bath temperature after 0.15 seconds.

A rapid temperature rise will cause large particles to fracture, thereby reducing the effective particle diameter and further shortening the heating-up time. The thermal shock of particles has been evidenced by investigations[30,31] on pyrolysis of brown coal in a shock tube. During the pyrolysis the concentration of hydrocarbons in the gas product changes when altering the heating rate, while the production of H_2 is not affected by these phenomena.[32] For the case described, the production of H_2 is expected immediately after the coal particles enter the liquid iron.

The dissolution of carbon in liquid iron is a diffusion-controlled process.[33,34] Consequently, the following relation applies to the dissolution of a carbon particle of radius r:

$$\frac{dr}{dt} = -\frac{M}{\rho} k_C\,(c^{\mathrm{sat}} - c) \qquad [9]$$

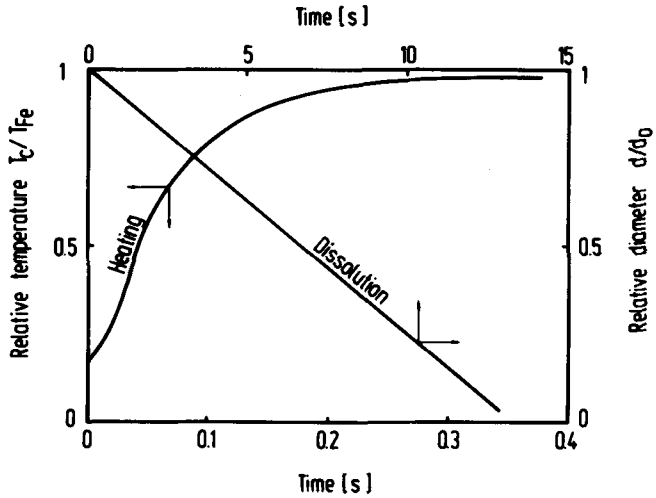

Fig. 6 — Course of heating-up and dissolution of a carbon (coal) particle of 1 mm diameter in the liquid iron bath with 3.5 wt pct C at 1773 K. T_c and T_{Fe} are the temperatures at the center of the particle and in the iron bath, respectively. d_0 is the initial particle diameter. Calculation parameters are given in the text.

where M and ρ are molecular weight and density of carbon, k_C is the mass-transfer coefficient, c^{sat} and c are the concentration of dissolved carbon at the carbon/melt interface and within the bulk melt, respectively. k_C can be determined using the following relation for dissolution of individual spheres subjected to a liquid flow:[35]

$$\mathrm{Sh} = 2 + 0.72\ \mathrm{Re}^{1/2}\,\mathrm{Sc}^{1/3} \qquad [10]$$

where Sh, Re, and Sc are the Sherwood, Reynolds, and Schmidt numbers, respectively. The course of dissolution of a carbon particle of 1 mm diameter is calculated using Eqs. [8] to [10] in combination with the equation of motion whereby the differential equations established were solved using appropriate numerical methods. According to these calculations 99.95 pct of the particle is dissolved within 13 seconds as shown in Figure 6. Particles with an initial diameter less than 0.1 mm diameter will be dissolved in less than 2 seconds according to Sh = 2.

The calculated dissolution time may be used to estimate the residence time of coal particles in the liquid iron. For a coal throughput of 500 kg/h per 1000 kg Fe-C alloy, the proportion of the undissolved coal particles with an initial diameter of 1 mm is estimated to be 0.14 wt pct. In the samples taken from the iron bath during gasification tests,[2] the concentration of undissolved carbon was found to be 0.1 wt pct, this being in satisfactory accord with the above estimate.

The carbon dissolution in iron is affected by dissolved oxygen as a result of simultaneous decarburization. As indicated by Eq. [9], the carbon dissolution rate increases with decreasing carbon concentration in the region surrounding the coal particle. Furthermore, the ascending CO bubbles induce an accelerated mass-transfer as a result of intensified convection.

Both oxygen and sulfur are surface active elements which decrease the surface tension of liquid iron considerably. The segregation of these elements at the carbon/liquid iron interface inhibits carbon dissolution.[36,37,38] This effect is important only if the rate of reaction at the interface is

less than the diffusion rate. However, such behavior does not apply to the case discussed here. For relatively small velocity differences between particle and melt, especially for residual decrepitated coal particles, the mass-transfer within the melt will be the rate-determining step for carbon dissolution.

B. *Reactions of Carbon and Oxygen*

By restricting the system in the reactor to the elements Fe, C, O, and H and species Fe, FeO, C_{sol}, $\underline{C}$ (dissolved), CO, CO_2, H_2, $\underline{H}$, H_2O, $\underline{O}$, and O_2, a number of reactions can be formulated. In this section the kinetics of the basic reactions are discussed and their relevance to the gasification process is assessed. Calculations using data acquired from investigations related to steelmaking form the basis of this discussion.

The reaction of solid carbon with gaseous oxygen

$$C_{sol} + \frac{1}{2}O_2 \longrightarrow CO, \qquad [11]$$

depends on the residence time of the coal particles in the gas space above the bottom tuyeres. During this short period (10^{-3} second), the particles do not attain the necessary temperatures and accordingly, reaction [11] takes place only to a limited extent. Even assuming a temperature of 1773 K and $P_{O_2} = 10^5$ Pa, the reaction rate of 10^{-4} mol cm^{-2} s^{-1} [39] converts a negligible 0.006 wt pct of the coal particles.

As is known from steelmaking processes, the reaction between oxygen and dissolved carbon in liquid iron is extremely fast. The decarburization rate of pig iron by top- or bottom-blowing of oxygen depends exclusively on the O_2 input at wt pct C $\leq$ 0.2.

The reaction rate during top-blowing of oxygen, as applied in the BOP (LD Process), is determined by the impact frequency of the O_2 molecules on the surface of the "hot spot".[40,41] This should also be true for the gas/liquid interface above the bottom tuyeres of the MIP reactor. The following reactions take place at this interface:

$$\frac{1}{2}O_2 \longrightarrow \underline{O} \qquad [12]$$

$$\frac{1}{2}O_2 + Fe \longrightarrow FeO \qquad [13]$$

$$\frac{1}{2}O_2 + \underline{C} \longrightarrow CO \qquad [14]$$

The observed high decarburization rate implies that the course of reactions [12] and [13] is not inhibited by the formation of an adherent layer of liquid FeO on Fe. But this is true only if the FeO layer is immediately removed by the turbulent flow ensuring a continuous adequate O_2/ Fe contact.

It is expected that O saturation of Fe at the interface will be reached very quickly due to the high oxygen potential, so that reaction [13] dominates more than [12]. The same also holds true for [14] since the concentration of C is considerably lower than that of Fe.

Considering established information,[15c,40–42] it is expected that the oxygen in the injection area is predominantly consumed according to reaction [13]. The prevailing turbulence causes the liquid oxide to be transported into the liquid bulk in dispersed form, where the following reactions then take place:

$$FeO \longrightarrow Fe + \underline{O} \qquad [15]$$

$$\underline{O} + \underline{C} \longrightarrow CO \qquad [16]$$

$$FeO + \underline{C} \longrightarrow Fe + CO \qquad [17]$$

$$FeO + CO \longrightarrow Fe + CO_2 \qquad [18]$$

$$CO_2 + \underline{C} \longrightarrow 2CO \qquad [19]$$

$$FeO + H_2 \longrightarrow Fe + H_2O \qquad [20]$$

$$H_2O + \underline{C} \longrightarrow H_2 + CO \qquad [21]$$

The dissolved oxygen, $\underline{O}$, generated initially as per reaction [12] but then formed predominantly by dissociation of FeO [15], continues to react essentially according to reaction [16]. Reaction [16] proceeds spontaneously *via* heterogenous nucleation,[43] which always occurs in liquid-iron bath reactors due to the presence of solid particles, liquid oxides, and gas bubbles.

Reaction [17], which constitutes the sum of [15] and [16], has been investigated experimentally.[44] Similarly, the reaction between liquid iron oxide and solid carbon has also been examined.[45] However, the results of those experiments enable only rough estimates to be made for the reaction rates. Based on the experimental information,[44,45] calculated times ranging between 30 and 175 seconds are obtained for a complete conversion of 3.3×10^{-3} g (4.7×10^{-5} mole) FeO, corresponding to the carbon content of a coal particle of 1 mm diameter. Neglecting dispersion effects, the contribution to the overall gasification process resulting from the direct reduction of FeO by dissolved and solid carbon will be extremely small. Reaction [17] is expected to take place predominantly *via* reactions [18] and [19], and [20] and [21]. The kinetics of liquid iron oxide reduction with CO and H_2 have been examined under defined conditions.[46,47] From the data reported by Nagasaka *et al.*,[46] the rate of reaction [18] is calculated to be 1.5×10^{-5} mol cm^{-2} s^{-1} at $T = 1773$ K and $P_{CO} = 10^5$ Pa. This results in a time of 0.2 second for the reduction of 4.7×10^{-5} mole FeO according to interfacial reaction [18], with the CO_2 formed corresponding to a bubble of 2.4 cm in diameter. As revealed by investigations,[48] reaction [19] is relatively fast. The CO_2 bubble of 2.4 cm diameter, will be converted to CO in the liquid Fe-C alloy at 1773 K within 2×10^{-3} s. For this calculation an average mass-transfer coefficient of 4.5×10^{-2} cm s^{-1} is determined according to the following relation:[49]

$$Sh = 1.13\ (Re\ Sc)^{1/2} \qquad [22]$$

The Re number based on the mean velocity of the ascending CO_2 bubble is calculated using a drag coefficient of 2.61.[50]

According to data in Reference 47, the rate of the interfacial reaction [20] is a factor of 100 greater than that of [18]. Reaction [21] is assumed to proceed as rapidly as reaction [19]. Although the amount of CO formed in the liquid iron bath is twice that of H_2, the above-mentioned kinetic data suggest that the contribution of reaction [20] to the FeO conversion will not be less important than that of [18]. If steam is injected as tuyere cooling gas or as an additional gasification agent, reaction [20] proceeds in the inverse direction, whereby high reaction rates are expected.

For an industrial 180 ton Q-BOP converter the decarburization rate is approximately 0.007 wt pct C s^{-1}.[15c] During tests using 5 ton-BOP (LD) converter decarburization rates of 0.027 wt pct C per second were achieved.[51] Transfer of this value to coal gasification in a liquid iron bath results in a coal throughput of 0.317 kg s^{-1} per 1000 kg Fe. This value is more than twice the coal throughput used during preliminary gasification tests.[2] Based on reported measurements of the circulation rate in gas-stirred liquids[52] and assuming a coal conversion efficiency of 95 pct, a coal throughput of 0.208 kg s^{-1} per 1000 kg Fe is considered feasible for the MIP coal gasification reactor.

IV. CONCLUSION

Thermodynamic calculations reveal that through the reaction of coal and oxygen in a liquid iron bath it is possible to produce a high-temperature gas consisting of CO and H_2 with a simultaneous transfer of the sulfur to a liquid slag phase.

A kinetic analysis of the reactions occurring in the liquid iron bath suggests that the oxygen reacts predominantly *via* an intermediate FeO formation. The FeO phase formed in the injection zone is widely dispersed in the liquid iron bath and rapidly decomposed by dissolution and subsequent reactions with dissolved carbon. When comparing all conceivable reactions, the dissolution of carbon is rate-determining for the overall gasification reaction.

Both the injected and the produced gases result in intense bath movement dispersing the coal particles and the other reactants, thus producing emulsion and foam states in the upper parts of the injection zone. The phenomena result in a significant increase in the mass transfer region and a lengthening of the retention time of the reactants in the liquid iron. This in turn explains the fast completion of reactions leading to the high conversion efficiency which is observed.

REFERENCES

1. E. A. Pelczarski and J. A. Karnavas: U.S. Patent 772791, 1968; German Patent 1955115, 1978.
2. P. Paschen, R. Pfeiffer, and K. -H. Waldhecker: *Glückauf*, 1981, vol. 117, no. 11a, pp. 14-16.
3. K. Brotzmann: *Stahl u. Eisen*, 1980, vol. 100, no. 10, p. 543.
4. Sumitomo Metal Industries, Ltd., Jap. Patent 164186-78, 1978; German Patent 2952434, 1984.
5. H. Nakajima, K. Okane, S. Furujo, S. Okamura, M. Sueyasu, T. Tanoue, S. Anezaki, and T. Matsuo: *Ironmaking and Steelmaking*, 1983, vol. 10, no. 3, pp. 130-35.
6. L. von Bogdandy, K. Brotzmann, H. -G. Fassbinder, E. Fritz, and F. Hoefer: *Stahl u. Eisen*, 1982, vol. 102, no. 7, pp. 341-46.
7. D. Radke, D. Neuschütz, and J. Hartwig: *Stahl u. Eisen*, 1979, vol. 99, no. 7, pp. 334-40.
8. J. Hartwig, D. Neuschütz, and D. Radke: *Stahl u. Eisen*, 1980, vol. 100, no. 10, pp. 535-43.
9. Kloeckner Werke AG: *Stahl u. Eisen*, 1981, vol. 101, no. 10, pp. 639-40.
10. I. Barin: Monograph on the Coal Gasification in Liquid Iron Bath, KHD Humboldt Wedag AG, Forschungs- und Entwicklungsberichte (Research and Development Reports), no. 1, 1986.
11. G. Eriksson: *Chem. Scr.*, 1975, vol. 8, pp. 100-03.
12. I. Barin and O. Knacke: *Thermochemical Properties of Inorganic Substances*, Springer Verlag, Berlin/Heidelberg/New York/Düsseldorf, 1973; Supplement with O. Kubaschewski, 1977.
13. D. R. Stull and H. Prophet: JANAF Thermochemical Tables, NSRDS-NBS 37, U.S. Dept. Commer., Washington, DC, 1971, Supplements 1974 to 1982.
14. L. S. Darken: *Trans. TMS-AIME*, 1967, vol. 239, pp. 90-96.
15. E. T. Turkdogan: *Physical Chemistry of High Temperature Technology*, Academic Press, New York, NY, 1980, pp. 60-88 (a), p. 282 (b), and p. 368 (c).
16. L. S. Darken and R. W. Gurry: *Physical Chemistry of Metals*, McGraw-Hill, New York, NY, 1953, p. 408.
17. F. Neumann and H. Schenck: *Arch. Eisenhüttenwes.*, 1959, vol. 30, no. 8, pp. 477-83.
18. A. Rist and J. Chipman: *Rev. Met.*, 1956, vol. 53, pp. 796-807.
19. F. D. Richardson and W. E. Dennis: *Trans. Faraday Soc.*, 1953, vol. 49, pp. 171-80.
20. C. W. Sherman, H. I. Elvander, and J. Chipman: *Trans. TMS-AIME*, 1950, vol. 188, pp. 334-40.
21. S. Ban-ya and J. Chipman: *Trans. TMS-AIME*, 1968, vol. 242, pp. 940-46.
22. J. P. Morris and R. C. Buehl: *Trans. TMS-AIME*, 1950, vol. 188, no. 2, pp. 317-22.
23. A. S. Venkatradi and H. B. Bell: *J. Iron Steel Inst.*, 1969, no. 8, p. 1110/1113.
24. K. Schwerdtfeger and H. G. Schubert: *Arch. Eisenhüttenwes.*, 1974, vol. 45, no. 7, pp. 437-39 and no. 8, pp. 449-507.
25. F. D. Richardson: *Physical Chemistry of Melts in Metallurgy*, Academic Press, London, 1974, p. 299.
26. E. T. Turkdogan: *Physicochemical properties of molten slags and glasses*, The Metals Society, London, 1983, p. 230 (a) and pp. 298-307 (b).
27. E. T. Turkdogan: U.S. Steel Corp., Monroeville, PA, private communication, 1984.
28. P. Grassmann: *Physikalische Grundlagen der Verfahrenstechnik, Salle + Sauerländer*, Frankfurt a. M. 1983, p. 599.
29. U. Grigull (Gröber/Erk/Grigull): *Die Grundgesetzte der Wärmeübertragung*, 3rd ed., Springer Verlag, Berlin/Heidelberg/New York, NY, 1981, pp. 55-64.
30. H. J. Frieske: "Schnelle Prolyse von pulverisierter Braunkohle in einem chemischen Stosswellenrohr," Dissertation, RWTH Aachen, 1982.
31. H. J. Frieske, E. Seelbach, and G. Adomeit: Institut für Allgemeine Mechanik, RWTH Aachen, paper presented at the 14th International Symposium on Shock Tubes and Waves, Sydney, 1983.
32. H. Juentgen and K. H. van Heek: *Brennstoff-Chemie*, 1969, vol. 50, no. 6, pp. 14-20.
33. O. Dahlke and O. Knacke: *Arch. Eisenhüttenwes.*, 1955, vol. 26, no. 7, pp. 373-78.
34. A. Mihajlovic and B. Marincek: *Arch. Eisenhüttenwes.*, 1973, vol. 44, no. 7, pp. 507-12.
35. P. N. Rowe, K. T. Claxton, and J. B. Lewis: *Trans. Inst. Chem. Engs.*, 1965, vol. 43, no. 1, pp. T14-31.
36. V. A. Grigoryan and V. P. Karshin: *Russian Metallurgy*, 1972, pp. 57-60.
37. K. Suzuki and N. Kayama: *Imono*, 1980, vol. 52, no. 7, pp. 389-93.
38. Y. Shigeno, M. Tokuda, and M. Ohtani: *J. Japan Inst. Metals*, 1982, vol. 46, no. 7, pp. 713-20.
39. R. R. Rajan and C. Y. Wen: *AIChE Journ.*, 1980, vol. 26, no. 4, pp. 642-55.
40. L. von Bogdandy: *Stahl u. Eisen*, 1965, vol. 85, no. 15, pp. 937-38.
41. O. Knacke: *Stahl u. Eisen*, 1965, vol. 85, no. 15, pp. 938-39.
42. G. H. Geiger, P. Kozakevitch, M. Olette, and P. V. Riboud: in *BOF Steelmaking*, J. M. Gaines, ed., 2nd printing, Iron and Steel Soc. of AIMMPE, Inc., Warrendale, PA, 1982, vol. 1, pp. 302-431.
43. L. von Bogdandy, H. -U. Hopp, and I. N. Stranski: *Arch. Eisenhüttenwes.*, 1966, vol. 37, no. 11, pp. 841-45.
44. S. K. Tarby and W. O. Philbrook: *Trans. TMS-AIME*, 1967, no. 7, pp. 1005-17.
45. Fay Fun: *Metall. Trans.*, 1970, vol. 1, no. 3, pp. 2537-41.
46. T. Nagasaka, Y. Iguchi, and S. Ban-ya: Tohoku University, Aza Aoba Aramaki, Sendai 980, Lecture no. S.761 presented at the 106th ISIJ Meeting, Oct. 1983.
47. S. Ban-ya, Y. Iguchi, and T. Nagasaka: Tohoku University, Aramaki

Aza Aoba, Sendai 982, Lecture no. S838, presented at the 104th ISIJ Meeting, Sept. 1982.
48. W. Loescher: *HOESCH Berichte aus Forschung und Entwicklung*, 1970, no. 2, pp. 43-52.
49. C. Hanson: *Recent Advances in Liquid-Liquid Extraction*, Pergamon Press, Oxford, 1971, p. 394.
50. H. Brauer: *Grundlagen der Einphasen- und Mehrphasenströmung*, Verlag Sauerlaender, Aarau/Frankfurt, 1971, p. 298.
51. K. Koch, J. Sittard, and P. Valentin: *Arch. Eisenhüttenwes.*, 1976, vol. 47, no. 10, pp. 583-88.
52. Y. Sahai and R. I. L. Guthrie: *Metall. Trans. B*, 1982, vol. 13B, pp. 193-202 and 203-11.